Weighted density-functional theory for simple fluids: Prewetting of a Lennard-Jones fluid

M. B. Sweatman
Department of Chemistry, Imperial College of Science, Technology and Medicine, Exhibition Road, London, SW7 2AZ, United Kingdom
(Received 19 December 2000; revised manuscript received 25 May 2001; published 5 December 2001)

The prewetting of a Lennard-Jones fluid is studied using weighted density-functional theory. The intrinsic Helmholtz free-energy functional is separated into repulsive and attractive contributions. An accurate functional for hard spheres is used for the repulsive functional and a weighted density-functional method is used for the attractive part. The results for this theory are compared against mean-field density-functional theory, the theory of Velasco and Tarazona [E. Velasco and P. Tarazona, J. Chem. Phys. **91**, 7916 (1989)] and grand canonical ensemble simulation results. The results demonstrate that the weighted density functional for attractive forces may offer a significant increase in accuracy over the other theories. The density-functional and simulation results also indicate that a previous estimate of the wetting temperature for a model of the interaction of argon with solid carbon dioxide, obtained from simulations [J. E. Finn and P. A. Monson, Phys. Rev. A, **39**, 6402 (1989)], is incorrect. The weighted density-functional method indicates that triple-point prewetting is observed for this model potential.

DOI: 10.1103/PhysRevE.65.011102 PACS number(s): 61.20.−p, 68.08.−p

I. INTRODUCTION

This paper continues the investigation of the performance of a weighted density-functional method for simple fluids. In previous work [1], this method was applied to supercritical adsorption of a Lennard-Jones (LJ) fluid in a slit pore, modeling the adsorption of ethane in a graphite slit, and was found to be more accurate than mean-field density-functional theory and in good agreement with simulation results. This paper demonstrates that this method, with some sensible modifications, may also perform well for subcritical fluids. In particular, it is shown that the prewetting surface phase transition is predicted more accurately by this method than by mean-field density-functional theory or the method of Velasco and Tarazona [2] for a model of the interaction of argon with solid carbon dioxide. Indeed, the results of this method are in good agreement with simulation results.

Prewetting has received much attention in recent decades, and there exist several excellent reviews [3]. Briefly, a line of prewetting transitions is thought to originate at a first-order wetting transition at the wetting temperature T_w and terminate at a surface critical point at a temperature T_{sc}. A prewetting transition is signalled by a discontinuous jump in adsorption as the chemical potential approaches the coexistence chemical potential, $\mu_{sat}(T)$, with the bulk fluid being gas. The jump in adsorption corresponds to a jump from a thin adsorbed film to a thick adsorbed film at the surface. After prewetting, the film thickness continues to increase as the chemical potential approaches $\mu_{sat}(T)$, and it eventually diverges at $\mu_{sat}(T)$.

For a review of the fundamentals of density-functional theory (DFT) and an introduction to this paper, the reader is referred to previous work [1] and other detailed accounts [4–6]. This paper proceeds as follows. The next section describes the theories employed, with particular attention devoted to the construction of the weighted density-functional theory method. These theories are then compared with simulation results for prewetting of a Lennard-Jones fluid modeling the interaction of argon with solid carbon dioxide. First, density profiles and adsorption isotherms are compared at a reduced temperature $T^*=k_BT/\epsilon=0.88$ (ϵ characterizes the argon-argon interaction strength, k_B is Boltzmann's constant). It is demonstrated that the weighted density-functional method is more accurate than the other theories in this test. Then the line of prewetting transitions for this model is determined. It is shown that the wetting temperature T_w predicted by density-functional theory is significantly below that predicted by Finn and Monson [7] from their simulations. They predicted $T_w^*=0.84\pm0.01$ for this system using NPTMC (constant pressure normal to the solid surface) simulation while DFT evidence from this paper indicates triple-point wetting, i.e., prewetting is observed at temperatures close to the triple-point temperature. By performing additional simulations for prewetting of a Lennard-Jones fluid at $T^*=0.75$, it is shown that, contrary to the claim of Finn and Monson, prewetting states for this model are thermodynamically stable for this temperature, i.e., that $T_w^*<0.75$, and that the wetting temperature predicted by Finn and Monson is incorrect. However, this paper does support the significant conclusion of the work of Finn and Monson and Fan and Monson [7,8], namely that prewetting transitions may be observed with Monte-Carlo simulations. This resolves earlier discussion [9,10] concerning this issue and also has consequences for other simulations of similar systems [11].

II. THEORY

For an introduction to the theory of this paper, see reference [1]. For each theory in this paper, the intrinsic excess Helmholtz free-energy functional is separated into repulsive and attractive contibutions

$$F[\rho(\vec{r})]=F_{rep}[\rho(\vec{r})]+F_{att}[\rho(\vec{r})]. \tag{1}$$

The LJ pair potential, ϕ_{LJ}, is separated according to the prescription of Woeks, Chandler, and Anderson (WDA) [12,1]. The repulsive functional is approximated by the fundamental

measure functional (FMF) for hard spheres of Rosenfeld and of Kierlik and Rosinberg [13]. The effective hard-sphere diameter d entering the hard-sphere functional is calculated according to the Barker-Henderson (BH) prescription [14,1].

A. Density-functional mean-field theory

Density-functional mean-field theory (DFMFT) is well known and details for this theory may be found in reference [1]. DFMFT may be derived from a perturbation expression

$$F = F_{rep} + \frac{1}{2}\int_0^1 d\alpha \int d\vec{r}_1 \int d\vec{r}_2 \rho(\vec{r}_1) \times \rho(\vec{r}_2) g^{(2)}(\vec{r}_1,\vec{r}_2;\phi_\alpha)\phi_{att}(r_{12}) \quad (2)$$

by setting $g^{(2)}(\vec{r}_1,\vec{r}_2;\phi_\alpha)=1$. This gives

$$F[\rho(\vec{r})] = F_{rep}[\rho(\vec{r});d] + \frac{1}{2}\int d\vec{r}_1 \int d\vec{r}_2 \rho(\vec{r}_1)\rho(\vec{r}_2)\phi_{att}(r_{12}). \quad (3)$$

For the Lennard-Jones fluid, the bulk-fluid equation of state (EOS) generated by DFMFT, with the repulsive functional approximated by the hard-sphere functional of Rosenfeld and Kierlik and Rosinberg and d given by the BH expression is not very accurate. For this reason, methods have been suggested that modify d [15,16] to improve the bulk EOS.

B. The method of Velasco and Tarazona

Another method for improving the bulk fluid equation of state generated by DFMFT at subcritical temperatures has been employed by Velasco and Tarazona [2]. They studied the adsorption of the Lennard-Jones fluid with an *ad hoc* form for an ''effective'' attractive interaction. By appealing to the perturbation expression (2), for the Lennard-Jones fluid they suggest that the ''effective'' attractive interaction be defined by

$$\begin{aligned}\phi_{att}(r) &= 0, \quad r \leqslant \lambda^{1/6}\sigma \\ &= 4\epsilon(\lambda(\sigma/r)^{12} - (\sigma/r)^6), \quad \lambda^{1/6}\sigma \leqslant r \leqslant r_c \\ &= 0, \quad r \geqslant r_c, \end{aligned} \quad (4)$$

where λ and d are determined to ensure that the bulk equation of state generated by the DFT yields accurate densities for coexisting liquid and gas. With this choice, $c^{(2)}_{att}(r)$ is the same for all fluid states on an isotherm, has a ''correlation hole'' for $r^* < \lambda^{1/6}$, and a minimum at $r^* = (2\lambda)^{1/6}$ of magnitude $-\epsilon/\lambda$. This method has been used to explore the prewetting transition of a Lennard-Jones fluid [10]. Because this approach is parametrized by fitting to reference thermodynamic data, it generally offers an improvement over DFMFT for thermodynamic quantities, such as the adsorption, for this problem. However, this is achieved at the expense of structural accuracy for dense fluids and it is not clear how this method can be adapted to a wider range of fluids or phenomena.

C. A weighted density method for attractive forces

Weighted density approximation (WDA) theories have previously been applied to the hard-sphere fluid [17–19]. The weighted density method that forms the focus of this paper is essentially a method for implementing a WDA-type functional for fluids for which an accurate equation of state is known but the pair-direct correlation function may be accurately determined by numerical methods only. It gives good results for super-critical adsorption of a Lennard-Jones fluid [1]. It is similar to the method of van Swol and Henderson [20], and there are also interesting parallels with the work of Kol and Laird and others [21] who investigate the freezing of soft spheres.

The WDA for the attractive functional is developed quite generally and could be used to describe both attractive and repulsive forces. However, it is recognized that the inherent approximations in the WDA method will generally not be as accurate for repulsive forces as established repulsive functionals [13,22,23], and so in this paper, the WDA method is applied to attractive forces only.

The excess Helmholtz free energy is approximated by a weighted density functional given by

$$F_{ex}[\rho(\vec{r})] = \int d\vec{r}\rho(\vec{r})\Psi_{ex}(\overline{\rho}(\vec{r})), \quad (5)$$

where Ψ_{ex} is the excess Helmholtz free energy per particle of a bulk fluid with density $\overline{\rho}$. The weighted density, $\overline{\rho}(r)$, is defined by

$$\overline{\rho}(\vec{r}_1) = \int d\vec{r}_2 \rho(\vec{r}_2) w(r_{12};\overline{\rho}(\vec{r}_1)), \quad (6)$$

where $w[r_{12};\rho(\vec{r}_1)]$ is a normalized, density-dependent weight function. The weight function is itself determined by requiring the functional to generate accurate pair-direct correlation functions for all uniform densities, i.e.,

$$\begin{aligned} -\beta^{-1}c^{(2)}(r_{12};\rho) = {} & \Psi'_{ex}\left(\frac{\delta\overline{\rho}(\vec{r}_1)}{\delta\rho(\vec{r}_2)} + \frac{\delta\overline{\rho}(\vec{r}_2)}{\delta\rho(\vec{r}_1)}\right) \\ & + \rho\Psi''_{ex}\int d\vec{r}_3 \frac{\delta\overline{\rho}(\vec{r}_3)}{\delta\rho(\vec{r}_1)}\frac{\delta\overline{\rho}(\vec{r}_3)}{\delta\rho(\vec{r}_2)} \\ & + \rho\Psi'_{ex}\int d\vec{r}_3 \frac{\delta^2\overline{\rho}(\vec{r}_3)}{\delta\rho(\vec{r}_1)\delta\rho(\vec{r}_2)}, \end{aligned} \quad (7)$$

where $'$ and $''$ indicate the first and second derivatives with respect to density and all quantities are evaluated for a uniform density.

By expanding Ψ_{ex}, $c^{(2)}(r)$, and $w(r;\rho)$ as power series in density, Eq. (7) may be solved to find $w(r;\rho)$. This is essentially the approach first used by Tarazona and Evans [18] in which terms up to second order in density were determined. When the bulk-fluid pair-direct correlation function can be determined approximately only at n nonzero density points (ρ_i with $i=0,\ldots,n$) the weight function may be approximated by an nth-order expansion in density

$$w(r;\rho)=\sum_{i=0}^{n}\rho^{i}w_i(r). \tag{8}$$

However, it becomes increasingly difficult to find the solution set of weight functions, w_i, as n increases. In this paper, two versions of the theory are presented. The first assumes a linear approximation for w, i.e.,

$$w(r;\rho)=w_0(r)+\rho w_1(r), \tag{9}$$

and this is the version that was used in previous work [1] concerning supercritical fluids. The second version assumes a quadratic approximation for w, i.e.,

$$w(r;\rho)=w_0(r)+\rho w_1(r)+\rho^2 w_2(r), \tag{10}$$

and this version forms the focus of this paper.

With an analytic approximation for Ψ_{ex} and with $c^{(2)}(r)$ determined approximately at n nonzero bulk densities, where $n=1$ for the first version and $n=2$ for the second version of the theory, the system of equations (7) and (8) may be solved at ρ_i. The weight functions for $n=1$ are given in Ref. [1]. For $n=2$, numerical methods are required to find the solution set w_i. The Newton-Raphson method is used to find the root of the equation for w_2,

$$[x_1+y_1w_2(k)+z_1w_2(k)^2]^{1/2}-[x_2+y_2w_2(k)+z_2w_2(k)^2]^{1/2}+u+vw_2(k)=0, \tag{11}$$

where

$$\begin{aligned}
u&=(b_2/2f_2)-(b_1/2f_1),\\
v&=(e_2/2f_2)-(e_1/2f_1),\\
x_i&=[-\beta c^{(2)}(k;\rho_i)-a_i+(b_i^2/4f_i)]/f_i,\\
y_i&=[(b_ie_i/2f_i)-d_i]/f_i,\\
z_i&=[(e_i^2/4f_i)-g_i]/f_i,
\end{aligned} \tag{12}$$

with

$$\begin{aligned}
a_i&=2\psi'(\rho_i)w_0(k)+\rho_i\psi''(\rho_i)w_0(k)^2,\\
b_i&=2\rho_i\psi'(\rho_i)+2\rho_i^2\psi''(\rho_i)w_0(k),\\
d_i&=2\rho_i^2\psi'(\rho_i)+2\rho_i^3\psi''(\rho_i)w_0(k),\\
e_i&=6\rho_i^3\psi'(\rho_i)+2\rho_i^4\psi''(\rho_i),\\
f_i&=2\rho_i^2\psi'(\rho_i)+\rho_i^3\psi''(\rho_i),\\
g_i&=4\rho_i^4\psi'(\rho_i)+\rho_i^5\psi''(\rho_i),
\end{aligned} \tag{13}$$

where $w_0(r)$ is given by

$$w_0(r)=-\beta c^{(2)}(r;\rho=0)/2\Psi'_{ex}(\rho=0), \tag{14}$$

$i=1,2$, and k indicates the Fourier-transformed quantity. For $k=0$, the solution $w_2(k=0)=0$ is enforced, and for $w_2(k+\Delta k)$ the solution for $w_2(k)$ is used as the initial point for the first iteration of the Newton-Raphson method (Δk is the k-space mesh spacing). $w_1(k)$ is determined from $w_2(k)$ by

$$w_1(k)=[x_1+y_1w_2(k)+z_1w_2(k)^2]^{1/2}-[b_1+e_1w_2(k)]/2f_1. \tag{15}$$

Finally, the remaining parameters ρ_i must be determined. In previous work, an *ad hoc* relation is suggested for the case when $n=1$,

$$\rho_1=\frac{\int d\vec{r}\,|\nabla\rho(\vec{r})|\overline{\rho(\vec{r})}}{\int d\vec{r}\,|\nabla\rho(\vec{r})|}. \tag{16}$$

This forces the functional to generate accurate $c^{(2)}(r)$ for uniform densities close to $\overline{\rho(\vec{r}')}$ where $\vec{r}'$ is the position in the fluid where the structure is most inhomogeneous. With this choice for ρ_1, the complete functional avoids reference to the bulk fluid that could lead to thermodynamic inconsistencies [24]. However, in this paper concerning prewetting, it is likely that ρ_1 defined by Eq. (16) will sometimes take on values between the bulk gas and liquid coexisting densities. This would have the consequence that the input $c^{(2)}_{att}(r;\rho_1)$ could be unobtainable, or inaccurate, for some fluid states. Instead, this paper fixes ρ_i to be equal to the coexisting gas, ρ_g, or liquid, ρ_l, densities. For $n=1$, two sets of results are obtained, one set with $\rho_1=\rho_g$ and the other with $\rho_1=\rho_l$. For $n=2$ results are obtained with $\rho_1=\rho_g$ and, initially, $\rho_2=\rho_l$.

In this paper, the functional described above is employed for the attractive functional of the LJ fluid only by exchanging all occurrences F_{ex}, Ψ_{ex}, and $c^{(2)}$ in Eqs. (5) to (15) with F_{att}, $\Psi_{att}=\Psi-\Psi_{PYHS}$, and $c^{(2)}_{att}=c^{(2)}-c^{(2)}_{PYHS}$, respectively, where PYHS denotes the Percus-Yevick hard-sphere quantity. These equations require that Ψ_{ex} is consistent with $c^{(2)}(r;\rho_1)$. However, there does not yet exist an accurate analytic EOS for the LJ fluid that is also consistent with accurate pair-direct correlation functions. To force a solution to Eqs. (14) to (15), the input $c^{(2)}_{att}(\rho_i)$ are manipulated by simply scaling them by an appropriate factor so that they do agree with Ψ_{att}. The presence of square-root terms indicates that Eqs. (14), (11), and (15) might not have real solutions for some fluid systems. However, in this paper no such difficulties are encountered for the LJ fluid.

So, the complete description for this WDA method is given by Eqs. (5) and (6), with Eq. (9), (14) and $\rho_1=\rho_g$ or $\rho_1=\rho_l$ for $n=1$, and Eqs. (10) and (11) to Eq. (15) with $\rho_1=\rho_g$ and (initially) $\rho_2=\rho_l$ for $n=2$. For $n=2$, the WDA method is similar to the approach of Tarazona and Evans for hard spheres [18], except that nonanalytic expressions for $c^{(2)}$ may be used as input. It would be an interesting exercise to apply the quadratic form of this WDA method to hard spheres and compare its performance with the hard-sphere functionals of Tarazona [18] and of Rosenfeld and Kierlik and Rosinberg [13].

III. PREWETTING OF A LENNARD-JONES FLUID

The above theories are tested by comparing their results for prewetting of a Lennard-Jones fluid against computer-simulation results. Fluid-fluid and solid-fluid potentials are chosen to be the same as those used by Finn and Monson and Fan and Monson [7,8], and comparison is made with their work. Apart from truncation, these potentials are the same as those used in earlier work by Ebner and Saam [25] and others [26].

The pair-potential parameters are chosen to model the interaction of argon with a solid carbon dioxide surface. Argon is modeled by a Lennard-Jones potential, truncated at $r_c^*=2.5$,

$$\phi(r)=4\epsilon\left[\left(\frac{\sigma}{r}\right)^{12}-\left(\frac{\sigma}{r}\right)^{6}\right], \quad r\leqslant r_c$$
$$=0, \quad r>r_c, \tag{17}$$

where σ and ϵ establish the length and energy scales of the potential. The carbon dioxide surface is modeled by a 9-3 potential, devoid of structure in the x and y directions,

$$V_{ext}(z)=\epsilon_w\left[\frac{2}{15}\left(\frac{\sigma_w}{z}\right)^{9}-\left(\frac{\sigma_w}{z}\right)^{3}\right], \quad z>0, \tag{18}$$

with values for the parameters $\sigma_w=1.0962\sigma$ and $\epsilon_w=2.643\epsilon$. This argon-solid carbon dioxide interaction model is used here as a ''toy'' model because of its popularity, the relative abundance of reference results and because its simplicity allows the focus of this paper to remain on the performance of the competing theories. Recently, another model potential for the interaction of argon with solid carbon dioxide has been proposed [27]. Mistura and co-workers claim that their model potential is more realistic than Eq. (18). They do not give details of their model potential, and so this paper continues to employ the earlier version (18). This is not important for the purposes of this paper provided theory and simulation employ the same model potential (18).

Finn and Monson [7] performed NPTMC simulations for the above model system at temperatures in the range $T^*=0.83$ to $T^*=1.0$. They estimated the wetting temperature to be $T_w^*=0.84\pm0.01$ and the prewetting critical temperature to be $T_{sc}^*=0.94\pm0.02$. At $T^*=0.88$, they observed prewetting to occur at a reduced pressure $P^*=P\sigma^3/\epsilon=0.0145\pm0.0005$ by observing a jump in adsorption from a thin to a thick film. Fan and Monson [8] subsequently perfomed NPTMC simulations for the same system at $T^*=0.88$ and also calculated the surface tension to determine the thermodynamic stability of the thin and thick films. They found that the thick prewetting film is thermodynamically stable for pressures between $P^*=0.0149\pm0.0005$ and the bulk saturation pressure. In this paper grand canonical ensemble Monte Carlo (GCEMC) simulations have been performed to confirm the results of Monson and coworkers. Monson and coworkers note that GCEMC simulations are expected to produce larger density fluctuations close to the prewetting transition than NPTMC simulations.

TABLE I. Gibbs ensemble results (Sim) compared against results from the equation of state (EOS) (19) for coexisting liquid and gas densities and pressure for the LJ fluid, truncated but not shifted at $r_c^*=2.5$. The numbers in brackets are statistical errors to 1 s.d. in the last digit.

T^*	ρ_g^* (Sim)	ρ_l^* (Sim)	P_g^* (Sim)	ρ_g^* (EOS)	ρ_l^* (EOS)	P_{sat}^* (EOS)
0.88	0.021(1)	0.722(2)	0.016(1)	0.0216	0.725	0.0165
0.75	0.0078(9)	0.797(3)	0.0054(7)	0.0069	0.793	0.0048

Application of the WDA method for attractive forces requires the definition of $\Psi_{att}(\rho)$ and $c_{att}^{(2)}(\rho_i)$ for the bulk fluid under consideration. In this paper, the equation of state of Kolafa and Nezbeda [28] is used together with a mean-field correction to account for truncation of the Lennard-Jones pair potential [1].

$$\Psi_{att}(\rho)=\Psi_{LJ}(\rho)-\Psi_{PYHS}(\rho;d)-\frac{\rho}{2}\int_{r_c}^{\infty}d\vec{r}\,\phi_{LJ}(r). \tag{19}$$

The Kolafa and Nezbeda EOS for the untruncated LJ fluid, Ψ_{LJ}, is accurate to within about 0.5% for P_{sat} over the range of temperatures studied in this paper. To assess the accuracy of the mean-field correction for truncation of the potential, the coexisting densities and pressure for the truncated LJ fluid have been calculated from Gibbs ensemble simulations [29] at $T^*=0.88$ and $T^*=0.75$. The results of these calculations are compared to the predictions of Eq. (19) in Table I. They indicate that Eq. (19) is sufficiently accurate.

In this paper, the reference hypernetted-chain (RHNC)-type integral equation closure [6] is employed to generate $c_{att}^{(2)}$, and a scaling method [using Eq. (7)] is used to enforce consistency, i.e.,

$$c_{att}^{(2)}(r;\rho_i)=[c_{RHNC}^{(2)}(r;\rho_i)-c_{PYHS}^{(2)}(r;\rho_i;d)]$$
$$\times\left(\frac{-2\beta\Psi'_{att}(\rho_i)-\beta\rho_1\Psi''_{att}(\rho_i)}{c_{RHNC}^{(2)}(k=0;\rho_i)-c_{PYHS}^{(2)}(k=0;\rho_i;d)}\right), \tag{20}$$

where $c_{RHNC}^{(2)}$ denotes the pair-direct correlation functions resulting from solution of the RHNC-type equation for the truncated potential (17). The RHNC-type integral equation is similar to that proposed by Rosenfeld [30] except that the BH prescription for d, rather than a prescription suggested by Rosenfeld [30], is used. It consists of solving the Ornstein-Zernike equation for a bulk fluid with an Euler-Lagrange closure where the bridge function is determined by the hard-sphere FMF of Rosenfeld and Kierlik and Rosinberg [13],

$$g^{(2)}(r;\rho_i)=\exp\left(-\beta(\phi(r)-\mu_{ex}^{HS}(\rho_i;d))+\int d\vec{r}(\rho(\vec{r})-\rho_i)\right.$$
$$\left.\times c_{att}^{(2)}(r;\rho_i)-\frac{\beta\delta F_{ex}^{HS}[\rho;d]}{\delta\rho(\vec{r})}\right). \tag{21}$$

TABLE II. GCEMC simulation results for a system modeling the interaction of argon on solid carbon dioxide at the reduced temperature $T^*=0.88$. The upper and lower sets correspond to simulations in which the initial configuration is an empty box and a thick-film state, respectively. N_{tot} and N_{run} are the total number of configurations and the number from which statistics are calculated, respectively. The corresponding density profiles are drawn in Fig. 1.

$\mathrm{Exp}(\beta\mu^*)$	ρ_b^*	P^*	$\Gamma^*=\Gamma\sigma^2$	$\gamma^*=\gamma\sigma^2/\epsilon$	$N_{tot}/10^6$	$N_{run}/10^6$
0.01	0.01143(3)	0.00936(3)	0.137(3)	0.085(4)	15	10
0.0115	0.0135(1)	0.01086(4)	0.185(3)	0.101(4)	5	4
0.013	0.0157(1)	0.01240(5)	0.27(2)	0.130(6)	5	4
0.014	0.0174(1)	0.01344(6)	0.36(2)	0.150(8)	5	4
0.0145	0.0178(1)	0.01398(6)	0.49(2)	0.163(9)	10	9
0.0148	0.01848(8)	0.01429(6)	0.63(6)	0.17(1)	20	10
0.0148	0.01848(8)	0.01429(6)	1.8(2)	0.16(3)	100	90
0.015	0.0189(1)	0.01450(6)	2.00(8)	0.18(2)	100	90
0.0155	0.0195(1)	0.01504(6)	2.60(8)	0.25(2)	100	90
0.016	0.0206(2)	0.01557(6)	3.5(2)	0.33(4)	100	90

Finally, the weight functions resulting from Eqs. (14) to (15) are truncated at r_c and rescaled to guarantee that the normalization conditions, $w_i(k=0)=\delta_{0i}$, are satisfied (δ is the Kronecker-delta function).

In all calculations planar symmetry is enforced, a grid of 50 points per σ is used and simple Picard iteration is employed to solve the respective Euler-Lagrange equations.

A. Simulation details

All GCEMC simulations in this paper are actually performed using a slit of width 20σ, with a hard wall opposing the solid carbon dioxide surface. Bulk gas properties are calculated from GCEMC simulations of the bulk fluid. Thin-film states are produced by initializing simulations with an empty box, while the thick-film states are produced by initializing simulations with thick-film configurations. Thick-film states typically involve more than five hundred particles. The bulk pressure and interfacial tension are calculated by integrating the Gibbs adsorption equation (see Ref. [1]) along a continuous branch of an isotherm. Integration constants are found at one point on each isotherm branch by calculating the pressure and interfacial tension from the ensemble-averaged microscopic pair-virial expression. Details of this method may be found in Refs. [31] and [8] for the pressure and interfacial tension, respectively.

B. Prewetting at $T^*=0.88$

In this section, the density profiles and adsorption isotherms for prewetting of a Lennard-Jones fluid adsorbed by a model 9-3 surface at a reduced temperature of $T^*=0.88$ are investigated. At this temperature, the equation-of-state (19) predicts the bulk liquid-gas transition at the reduced saturation pressure $P^*_{sat}=0.0165$. The corresponding liquid and gas densities are $\rho^*_l=\rho_l\sigma^3=0.725$ and $\rho^*_g=0.0216$, respectively. This compares with $P^*_{sat}=0.0157$ predicted by Finn and Monson [7] using a modified Nicolas *et al.* EOS [32].

Grand canonical ensemble simulation has been used to reproduce the results of Finn and Monson for the prewetting transition at $T^*=0.88$. The simulation parameters and results are given in Table II. Construction of interfacial tension isotherms for the thin- and thick-film branches shows that prewetting occurs at $P^*=0.0145\pm0.0005$, i.e., $\rho^*=0.0189\pm0.0007$. This is in good agreement with the result of Fan and Monson, $P^*=0.0149\pm0.0005$. The results for density profiles corresponding to the results in Table II are shown in Fig. 1 (note that the thin-film states at $P^*=0.0141$ and $P^*=0.0145$ require large simulations with about 1000 particles to obtain stable thin films). These results are in good agreement with the simulations of Finn and Monson and Fan and Monson, with the location and height of successive peaks and troughs in the density profiles bearing close resemblance to theirs. The density profiles shown may be grouped into those with liquidlike density in at least the second layer adjacent and normal to the wall (the thick-film prewetting states) and those with gaslike density in the second layer (the thin-film states). They clearly show a jump in adsorption, from approximately one to three liquidlike layers, as the bulk

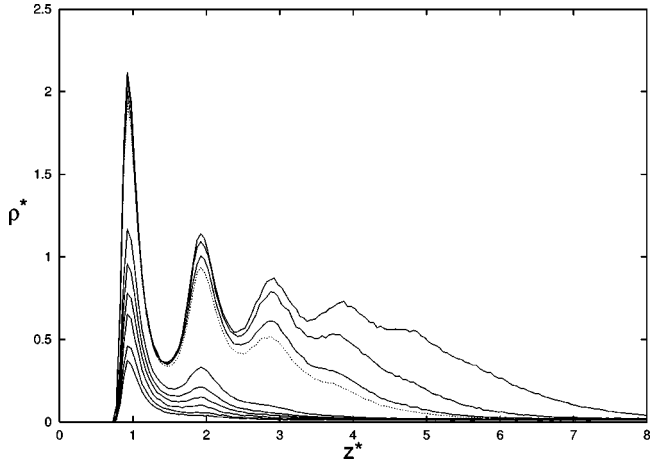

FIG. 1. Reduced density profiles for a system modeling the interaction of argon on solid carbon dioxide at the reduced temperature $T^*=0.88$. The density profiles correspond to GCEMC simulation results shown in Table II. The dashed line is a metastable state.

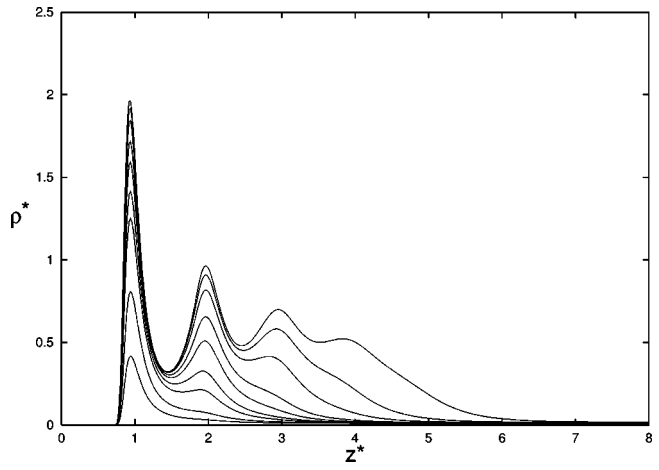

FIG. 2. As in Fig. 1, except that the density profiles correspond to DFMFT results shown in Table III.

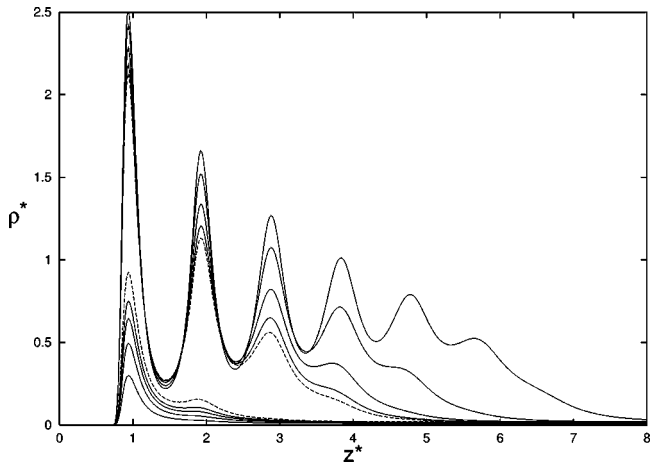

FIG. 3. As in Fig. 1, except that the density profiles correspond to results obtained from the theory of Velasco and Tarazona shown in Table IV. Dashed lines are metastable states.

pressure is increased towards the saturation pressure. They also show that the prewetting states have structure normal to the wall on a length scale similar to σ, and that this structure decays with distance from the wall.

The density profiles for this system resulting from the DFMFT treatment of attractive forces are shown in Fig. 2. It shows a series of density profiles corresponding to a series of pressures approaching the bulk saturation pressure, with $P^*_{sat}=0.0141$ using this theory. The corresponding coexisting bulk liquid and gas densities are $\rho^*_l=0.622$ and $\rho^*_g=0.0183$, respectively. Table III gives the corresponding thermodynamic results. It demonstrates that this theory does not predict the prewetting transition at $T^*=0.88$, although the adsorption does rise steeply in the region of $P^*=0.0109$, which corresponds to $\rho^*=0.0135$. Instead, the adsorption increases smoothly as the pressure is increased towards saturation, which indicates that this temperature is super critical of the prewetting critical temperature for this theory. Figure 2 shows that DFMFT gives a reasonable account of the structure in the liquidlike film adjacent and normal to the wall, although the density of this film is generally lower than that observed in Fig. 1.

The density profiles for this system resulting from the method of Velasco and Tarazona, with $d^*=d/\sigma=0.9703$ and $\lambda=0.6566$, are shown in Fig. 3. It shows a series of density profiles corresponding to a series of bulk pressures approaching the bulk saturation pressure, with $P^*_{sat}=0.0163$ using this theory. The corresponding coexisting bulk liquid and gas densities are $\rho^*_l=0.725$ and $\rho^*_g=0.0208$, respectively. Table IV gives the corresponding thermodynamic results. It demonstrates that this theory predicts the prewetting transition at $P^*=0.0140$, which corresponds to $\rho^*=0.0176$. Figure 3 also shows that the theory is unable to accurately reproduce the structure in the liquidlike film adjacent and normal to the wall. This is because the theory over-emphasizes pair correlations in dense fluids.

The density profiles for this system resulting from the WDA method with $n=1$ are shown in Fig. 4. It shows two series of density profiles corresponding to a series of bulk pressures approaching the bulk saturation pressure, with $P^*_{sat}=0.0165$ using this theory. The corresponding coexisting bulk liquid and gas densities are $\rho^*_l=0.725$ and $\rho^*_g=0.0216$, respectively. The two sets of results correspond to the two choices for ρ_1, i.e., $\rho_1=\rho_g$ (dashed lines) and ρ_1

TABLE III. DFMFT results for a system modeling the interaction of argon on solid carbon dioxide at the reduced temperature $T^*=0.88$. The coresponding density profiles are drawn in Fig. 2.

ρ^*_b	P^*	$\mu^*=\mu\sigma^3/\epsilon$	Γ^*	γ^*
0.01	0.00826	−4.16	0.151	0.082
0.012	0.00979	−4.02	0.321	0.111
0.013	0.01053	−3.96	0.576	0.137
0.0133	0.01075	−3.94	0.719	0.148
0.0135	0.0109	−3.93	0.93	0.157
0.014	0.01127	−3.91	1.133	0.185
0.015	0.012	−3.86	1.494	0.25
0.016	0.01271	−3.81	1.871	0.328
0.017	0.01341	−3.77	2.432	0.418

TABLE IV. DFT results for a system modeling the interaction of argon on solid carbon dioxide at the reduced temperature $T^*=0.88$ using the theory of Velasco and Tarazona. The corresponding density profiles are drawn in Fig. 3.

ρ^*_b	P^*	μ^*	Γ^*	γ^*
0.01	0.00833	−4.146	0.1048	0.072
0.014	0.01141	−3.887	0.1859	0.1083
0.016	0.01289	−3.788	0.2546	0.1297
0.017	0.01362	−3.744	0.3082	0.142
0.018	0.01434	−3.703	0.4034	0.1564
0.0173	0.01384	−3.731	1.69	0.1312
0.0175	0.01398	−3.723	1.828	0.1456
0.018	0.01434	−3.703	2.135	0.1856
0.019	0.01505	−3.664	2.786	0.2797
0.02	0.01575	−3.628	3.88	0.3971

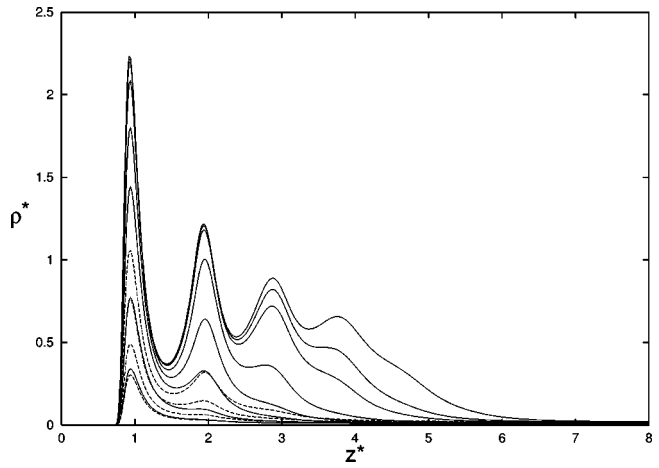

FIG. 4. As in Fig. 1 except that the density profiles correspond to results obtained from the WDA method with $n=1$ shown in Table V. Solid lines correspond to the choice $\rho_1=\rho_l$ and dashed lines to $\rho_1=\rho_g$.

$=\rho_l$ (solid lines). Table V gives the two corresponding sets of thermodynamic results. The results with $\rho_1=\rho_g$ show the adsorption increasing smoothly to a relatively small value at bulk saturation. The results with $\rho_1=\rho_l$ show the adsorption increasing smoothly as the pressure approaches saturation. Figure 4 shows that with $\rho_1=\rho_g$, the theory is able to produce density profiles in reasonable agreement with the simulation thin-film profiles, but is unable to account for the thick film. This is because pair correlations in a dense fluid cannot be accurately obtained by extrapolation about those at ρ_g. Conversely, with $\rho_1=\rho_l$, the theory is able to produce density profiles in good agreement with the thick-film simulation profiles, but is unable to accurately account for the thin film. Indeed, the theory with $\rho_1=\rho_l$ produces qualititively similar results to DFMFT, i.e., neither theory is sufficiently accurate for low-density fluids in this prewetting test.

TABLE V. DFT results for a system modeling the interaction of argon on solid carbon dioxide at the reduced temperature $T^*=0.88$ using the WDA method with $n=1$. The upper and lower sets correspond to $\rho_1=\rho_g$ and $\rho_1=\rho_l$, respectively. The corresponding density profiles are drawn in Fig. 4.

ρ_b^*	P^*	μ^*	Γ^*	γ^*
0.01	0.00827	−4.159	0.109	0.0731
0.014	0.01128	−3.905	0.1931	0.1098
0.018	0.01411	−3.727	0.3475	0.1557
0.021	0.01613	−3.623	0.5859	0.2023
0.01	0.00827	−4.159	0.1229	0.0755
0.013	0.01054	−3.96	0.3152	0.1108
0.014	0.01128	−3.905	0.7003	0.141
0.015	0.012	−3.855	1.04	0.183
0.016	0.01272	−3.809	1.515	0.2434
0.018	0.01411	−3.727	2.103	0.3928
0.019	0.0148	−3.69	2.403	0.4756
0.02	0.01547	−3.656	2.845	0.5656

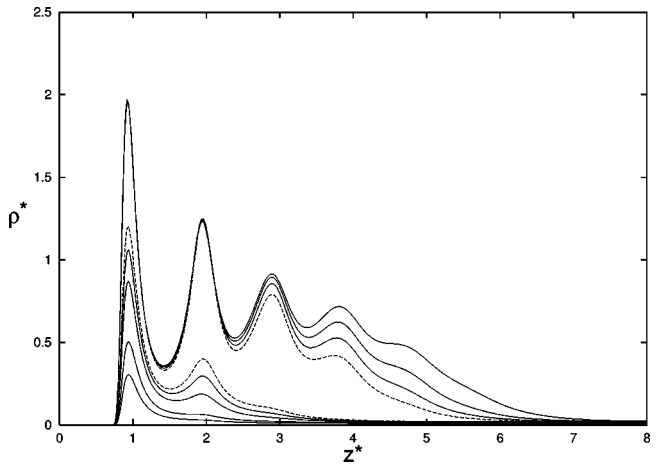

FIG. 5. As in Fig. 1 except that the density profiles correspond to results obtained from the WDA theory with $n=2$, $\rho_1=\rho_g$, $\rho_2=\rho_l$ shown in Table VI. Dashed lines are metastable states.

The density profiles for this system resulting from the WDA method with $n=2$ are shown in Fig. 5. It shows a series of density profiles corresponding to a series of bulk pressures approaching the bulk saturation pressure, with $P_{sat}^*=0.0165$ using this theory. The corresponding coexisting bulk liquid and gas densities are $\rho_l^*=0.725$ and $\rho_g^*=0.0216$, respectively. Table VI gives the corresponding thermodynamic results. It demonstrates that this theory predicts the prewetting transition at $P^*=0.0149$, which corresponds to $\rho^*=0.0192$. This is in good agreement with the simulation results of this paper and the work of Monson and coworkers. Figure 5 also shows that the theory is able to reproduce the structure in the thick and thin films adjacent and normal to the wall with good accuracy.

Figure 6 compares the adsorption isotherms resulting from simulation and the five theories described above. The WDA method produces an adsorption isotherm in good agreement with the simulation. Small differences may be seen in the neighborhood of the the prewetting transition. The theory of Velasco and Tarazona predicts the prewetting transition, but it is predicted to occur at a lower pressure and the adsorption in the thick film is over estimated. The other

TABLE VI. DFT results for a system modeling the interaction of argon on solid carbon dioxide at the reduced temperature $T^*=0.88$ using the WDA method with $n=2$, $\rho_1=\rho_g$, and $\rho_2=\rho_l$. The corresponding density profiles are drawn in Fig. 5.

ρ_b^*	P^*	μ^*	Γ^*	γ^*
0.01	0.00827	−4.159	0.1095	0.0732
0.014	0.01128	−3.905	0.1985	0.1104
0.018	0.01411	−3.727	0.4158	0.1602
0.019	0.0148	−3.69	0.565	0.178
0.0195	0.01513	−3.673	0.6964	0.1889
0.019	0.0148	−3.69	2.227	0.1658
0.0195	0.01513	−3.673	2.482	0.2071
0.02	0.01547	−3.656	2.751	0.2513
0.0205	0.0158	−3.639	3.109	0.2992

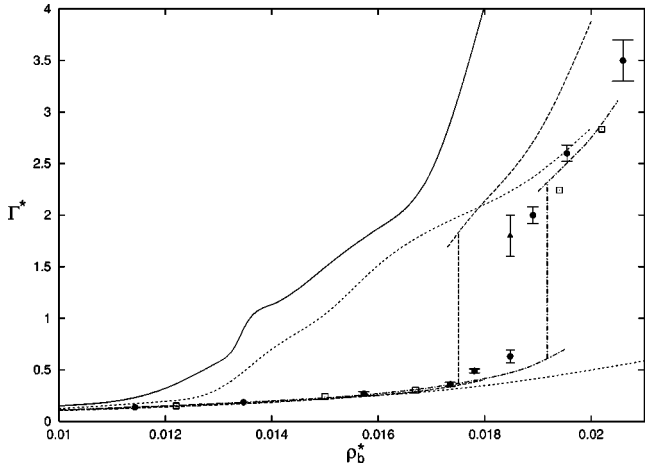

FIG. 6. Reduced adsorption isotherms corresponding to the results in Figs. 1–5 and Tables II–IV. Solid symbols correspond to the results in Fig. 1 and Table II. The triangle denotes a metastable state. Open symbols are the NPTMC results of Fan and Monson [8]. The solid, long-dashed, short-dashed and dash-dotted lines correspond to the results in Figs. 2, 3, 4, 5 and Tables III, IV, V, and VI, respectively.

theories fail to predict the prewetting transition at this reduced temperature, but the WDA method with $n=1$ and $\rho_1=\rho_l$ is accurate for the thick film. A clear difference between all the DFT results and the simulation results is the rate of decay of thick-film density to the bulk gas density with increasing distance from the wall. It has been speculated that this difference is due to the influence of capillary waves [10].

C. The prewetting line

An important feature of the WDA method of this paper is the choice for ρ_i. In the preceding section, it was demonstrated that the choice $\rho_1=\rho_g$ and $\rho_2=\rho_l$ leads to prediction of the prewetting transition $P^*=0.0149$ ($\rho^*=0.0192$) at $T^*=0.88$. This compares to the simulation result of Fan and Monson of $P^*=0.0149\pm0.0005$ and the simulation result of this paper, $P^*=0.0145\pm0.0005$ ($\rho^*=0.0189\pm0.0007$). But for the remainder of this paper, the choice $\rho_2=\rho_m=(\rho_l+\rho_{sl})/2$ is used where ρ_{sl} is the liquidlike spinodal density. This choice is used because $\bar{\rho}$ is generally between ρ_l and ρ_{sl} in the thick film. Thus, using $\rho_2=\rho_l$ is likely to be less accurate than $\rho_2=\rho_m$. With this choice for ρ_2, prewetting at $T^*=0.88$ is predicted at $P^*=0.0147$, which corresponds to $\rho^*=0.0189$. These results are still within the simulation errors. The density profiles corresponding to the results in Table VII are not shown since they are almost indistinguishable from those in Fig. 5 on the scale used. For temperatures lower than $T^*=0.88$, the agreement between simulation and theory is improved by the use of $\rho_2=\rho_m$ compared to $\rho_2=\rho_l$.

Figure 7 shows the location of the line of prewetting transitions predicted with DFMFT and the WDA method down to $T^*=0.7$. Given that the critical temperature of argon is 150.9 K [34], and the critical temperature for the Lennard-Jones fluid predicted by the EOS (19) is $T_c^*=1.21$, then the triple point of argon ($T_t^{Ar}=83.8$ K [27]) corresponds to $T_t^*=0.67$ with this EOS. The range of validity of this EOS is $0.68<T^*<20$ [28]. With DFMFT, the critical temperature is predicted to be $T_c^*=1.30$, and hence, the triple-point temperature is estimated to be $T_t^*=0.72$ within this theory. Thus, $T^*=0.7$ is expected to be close to the triple point of argon and lower temperatures are not investigated.

TABLE VII. DFT results for a system modeling the interaction of argon on solid carbon dioxide at the reduced temperature $T^*=0.88$ using the WDA method with $n=2$, $\rho_1=\rho_g$, and $\rho_2=\rho_m$.

ρ_b^*	P^*	μ^*	Γ^*	γ^*
0.01	0.00827	−4.159	0.1095	0.0732
0.014	0.01128	−3.905	0.1989	0.1104
0.018	0.01411	−3.727	0.4252	0.1607
0.019	0.0148	−3.69	0.5986	0.1791
0.0195	0.01513	−3.673	0.7828	0.191
0.0185	0.01446	−3.708	2.059	0.1437
0.019	0.0148	−3.69	2.301	0.1834
0.0195	0.01513	−3.673	2.509	0.2255
0.02	0.01547	−3.656	2.74	0.2699
0.0205	0.0158	−3.639	3.067	0.3172

With both of these approaches, prewetting is observed in the region of the triple point of argon and so this model potential for argon on solid carbon-dioxide is said to exhibit triple-point prewetting. The prewetting surface critical temperature T_{sc} is found to be $T_{sc}^*=1.01\pm0.01$ and 0.83 ± 0.01 for the WDA method and DFMFT, respectively. From their NPTMC simulations, Finn and Monson predict the line of prewetting transitions to begin at $T_w^*=0.84\pm0.01$ and end at $T_{sc}^*=0.94\pm0.02$. The theory of Velasco and Tarazona pre-

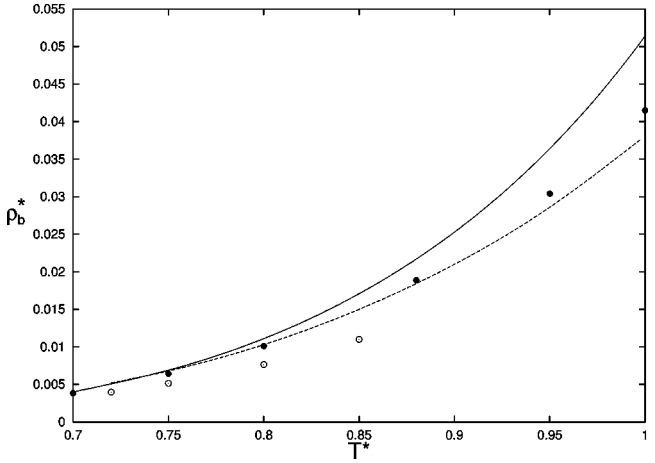

FIG. 7. The prewetting behavior of a model of argon on solid carbon dioxide predicted by DFT. The solid line and solid symbols correspond to the coexisting bulk gas density and the bulk gas density at which prewetting occurs, respectively, as predicted by the WDA method with $n=2$, $\rho_1=\rho_g$, and $\rho_2=\rho_m$. The dashed line and open symbols correspond to the coexisting bulk gas density and the bulk gas density at which prewetting occurs, respectively, as predicted by DFMFT.

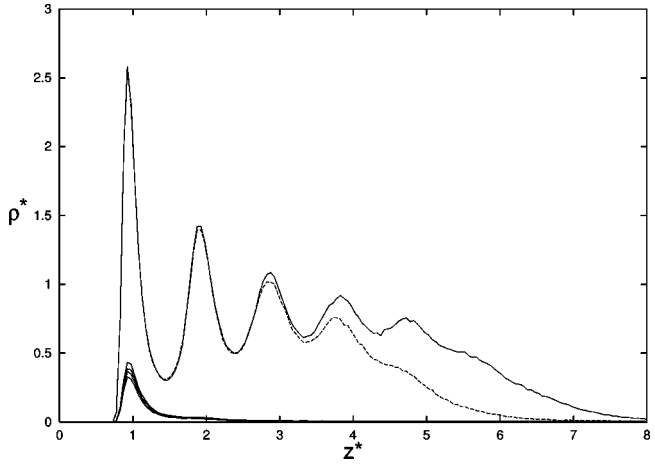

FIG. 8. Reduced density profiles for a system modeling the interaction of argon on solid carbon dioxide at the reduced temperature $T^*=0.75$. The density profiles correspond to GCEMC simulation results shown in Table VIII. The dashed line is a metastable state.

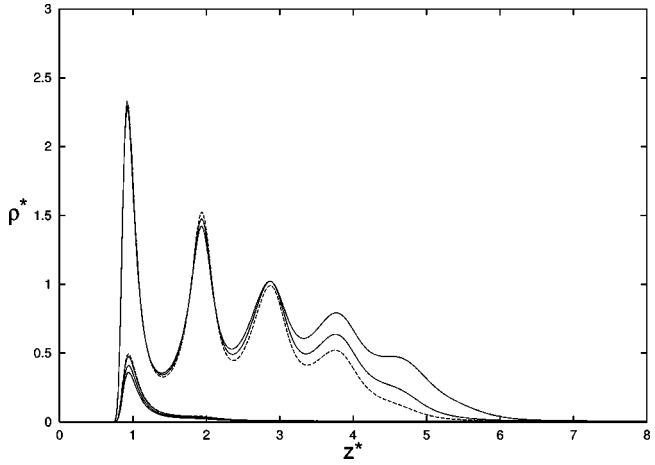

FIG. 9. As in Fig. 8, except that the density profiles correspond to results obtained from the WDA theory with $n=2$, $\rho_1=\rho_g$, $\rho_2=\rho_m$ shown in Table IX. Dashed lines are metastable states.

dicts $T_w^*=0.75$ and $T_{sc}^*=0.96$ [7]. The difference in the results obtained by the theory of Velasco and Tarazona and the simulations of Finn and Monson for these quantities motivated some comments [9] concerning the accuracy of the NPTMC simulations of Finn and Monson, and in particular, the bulk equation of state, due to Nicolas *et al.* [32], used to determine bulk liquid-gas coexistence.

The above DFT results provide similar motivation in this paper for the search for prewetting states at temperatures below the wetting temperature given by Finn and Monson, $T_w^*=0.84\pm0.01$. Figure 8 shows the results for density profiles at $T^*=0.75$, produced by GCEMC simulations. The corresponding thermodynamic results are shown in Table VIII. Construction of interfacial tension isotherms for the thin- and thick-film branches shows that prewetting occurs at $P^*=0.0045\pm0.0001$, i.e., $\rho^*=0.0064\pm0.0002$. This pressure is less than the bulk liquid-gas coexistence pressure displayed in Table I. Density profiles resulting from the WDA method at $T^*=0.75$ are shown in Fig. 9 and correspond to the results in Table IX. Comparison with Fig. 8 demonstrates that this theory is accurate for density profiles at this low temperature. The prewetting pressure predicted by the WDA theory is $P^*=0.00458$. Thus, the WDA method has accurately predicted a prewetting transition for this model at $T^*=0.75$.

These results indicate that there is a significant free-energy barrier between these thin-film and thick-film states that is statistically unlikely to be crossed during typical GCEMC simulations at $T^*=0.75$ unless the pressure is sufficiently far from the prewetting pressure. The results also indicate that the estimate for T_w of Finn and Monson is incorrect. Finn and Monson describe that at $T^*=0.83$, a thick film is not observed at $P^*=0.01$, which is close to the saturation pressure obtained from the modified EOS of Nicolas *et al.*, $P_{sat}^*=0.0103$. The modified EOS of Nezbeda and Kolafa yields $P_{sat}^*=0.0108$ at this temperature. The weighted density-functional method predicts prewetting at $P^*\approx0.01$ at this temperature. Finn and Monson also describe that they start their NPTMC simulations from final configurations obtained at lower pressure (or a uniform distribution of particles if no such state is simulated). In the light of the above results, at $T^*=0.75$ it is likely that $P^*=0.01$ is not sufficiently close to the saturation pressure at $T^*=0.83$ to observe thick-film formation unless the simulation is initialized with a thick-film configuration. To support

TABLE VIII. GCEMC simulation results for a system modeling the interaction of argon on solid carbon dioxide at the reduced temperature $T^*=0.75$. The upper and lower sets correspond to simulations in which the initial configuration is an empty box and a thick-film state, respectively. The corresponding density profiles are drawn in Fig. 9.

$\mathrm{Exp}(\beta\mu^*)$	ρ_b^*	P^*	Γ^*	γ^*	$N_{tot}/10^6$	$N_{run}/10^6$
0.005	0.00548(3)	0.00391(2)	0.111(3)	0.060(1)	5	4
0.0052	0.00572(3)	0.00407(2)	0.123(3)	0.063(1)	5	4
0.0054	0.00593(3)	0.00424(2)	0.135(3)	0.067(1)	5	4
0.0056	0.00621(3)	0.00440(2)	0.150(3)	0.071(1)	20	5
0.0056	0.00621(3)	0.00440(2)	3.18(7)	0.03(6)	100	90
0.0058	0.00646(3)	0.00456(2)	4.2(2)	0.13(6)	100	90

TABLE IX. DFT results for a system modeling the interaction of argon on solid carbon dioxide at the reduced temperature $T^*=0.75$ using the WDA method with $n=2$, $\rho_1=\rho_g$, and $\rho_2=\rho_m$. The corresponding density profiles are drawn in Fig. 9.

ρ_b^*	P^*	μ^*	Γ^*	γ^*
0.0056	0.00401	−3.957	0.1203	0.06215
0.006	0.00428	−3.91	0.1397	0.06822
0.0064	0.00455	−3.866	0.1646	0.07481
0.0065	0.00462	−3.856	0.1721	0.07656
0.0064	0.00455	−3.866	2.503	0.06543
0.0065	0.00462	−3.856	2.7525	0.09253
0.00655	0.00465	−3.851	3.64	0.1074

this conclusion, two further GCEMC simulations have been performed at $T^*=0.83$ and $P^*=0.01$, one initilized with a thin-film configuration and the other with a thick-film configuration. The results of these simulations are presented in Table X. They indicate that metastable thin and thick films do exist at this temperature and pressure, although it cannot be decided which state is stable from these results alone.

Using the WDA DFT results as a guide, they suggest that triple-point prewetting is observed for this model potential. The WDA method predicts T_{sc} to be higher than predicted by the other theories or by Finn and Monson from their NPTMC simulations. It should be noted that it is difficult to accurately predict T_{sc} from simulations since fluctuations in a relatively small (in directions parallel to the surface) simulation box will tend to mask the occurrence of distinct thin and thick films, just as finite-size effects tend to mask the location of the bulk critical point in Gibbs ensemble simulations of bulk coexisting phases.

IV. CONCLUSION

The WDA method with $n=2$ for attractive interactions has been shown to be significantly more accurate than MFDFT and the method of Velasco and Tarazona for prewetting of a model of the interaction of argon with solid carbon dioxide. Indeed, the accuracy of the WDA theory cast doubt on some results obtained from earlier NPTMC simulations [7,8] of the same system. Additional GCEMC simulations in this paper demonstrate that the WDA theory is accurate and that these earlier results for prewetting are likely to be incorrect for $T^*<0.84$. The WDA method and GCEMC simulations indicate that triple-point prewetting is observed for this system. The error in the earlier results probably stems both from the use of the Nicolas equation-of-state for the LJ fluid and the neglect to perform sufficient simulations initialized from thick-film states. The GCEMC simulations in this paper demonstrate that by choosing different initial configurations, thick- and thin-film fluid states may be simulated at the same chemical potential and temperature. Clearly, care must be exercised when performing simulations where meta-stable states exist. However, this paper supports the general and significant result of Monson and coworkers that prewetting may be observed with Monte Carlo simulations. It is expected that the accuracy of the WDA method will extend to other systems when the corresponding input data (bulk equation of state, and bulk pair-direct correlation functions at two nonzero densities) and the quadratic approximation for w (10) are sufficiently accurate. Previous work [1] has shown that the theory (with $n=1$) is accurate for super-critical adsorption of a Lennard-Jones fluid. The investigations in this and previous work [1] involve significant adsorption and are therefore demanding tests of the relevent theories. It would be interesting to examine the performance of other density-functional methods [34] for the same fluid systems.

Another model potential for the interaction of argon with solid carbon dioxide has been proposed recently [27]. This model includes surface heterogeneity in the directions normal to the wall, and the laterally averaged interaction strength is stronger than for the model potential described by Eq. (18). It would be interesting to determine the surface phase behavior for this model using the WDA method.

A deficiency of the WDA method for attractive forces is the lack of a consistent and theoretically motivated choice for the interpolation densities, ρ_i. In previous work concerning super-critical adsorption [1], the choice (16) was demonstrated to be reasonable. In this paper, to avoid the possibility of ρ_i entering the unstable spinodal region of the bulk fluid, the interpolation densities are fixed outside this region. This also has the desirable consequence that ρ_i is independent of ρ_b (if ρ_i was dependent on ρ_b then additional terms involving $\delta\rho_i/\delta\rho(\vec{r})$ would appear in the Euler-Lagrange equation [1]). These problems arise because the method attempts to map local (weighted) properties of the inhomogeneous fluid onto properties of an appropriate bulk fluid. The FMF of Rosenfeld and others [13] avoids these problems by using fundamental geometric and dimensional arguments. The FMF functional has recently been extended to more general spherical pair potentials [35] and to parallel hard cubes [36]. It would be interesting to compare the accuracy of this FMT approach [35] with the WDA method in this paper for a range of systems and states.

TABLE X. GCEMC simulation results for a system modeling the interaction of argon on solid carbon dioxide at the reduced temperature $T^*=0.83$. The upper and lower sets correspond to simulations in which the initial configuration is an empty box and a thick-film state, respectively.

$\mathrm{Exp}(\beta\mu^*)$	ρ_b^*	P^*	Γ^*	γ^*	$N_{tot}/10^6$	$N_{run}/10^6$
0.01105	0.01322(7)	0.0100(6)	0.49(2)	0.13(2)	10	5
0.01105	0.01322(7)	0.0100(6)	2.70(3)	0.18(7)	10	5

It would also be interesting to apply the WDA method in the test-particle limit, i.e., $V_{ext}(\vec{r}) = \phi(r)$, and to compare its results against those of established bulk fluid integral equation theories. The pair-direct correlation function could be used iteratively as input into the WDA method. In this instance, the WDA method would essentially provide a recipe for calculating the attractive contribution to the bridge function.

[1] M. B. Sweatman, Phys. Rev. E **63**, 031102 (2001).
[2] E. Velasco and P. Tarazona, J. Chem. Phys. **91**, 7916 (1989).
[3] See, for example, *Fluid Interfacial Phenomena*, edited by C. A. Croxton (Wiley, New York, 1986); *Fundamentals of Inhomogeneous Fluids*, edited by D. Henderson (Wiley, New York, 1992); S. Dietrich, in *Phase Transitions and Critical Phenomena*, edited by C. Domb and J. L. Lebowitz (Academic, New York, 1988), Vol. 12.
[4] For a review, see R. Evans, in *Fundamentals of Inhomogeneous Fluids* (Ref. [3]).
[5] R. Evans, Adv. Phys. **28**, 143 (1979).
[6] J. P. Hansen and I. R. McDonald, *Theory of Simple Liquids*, 2nd ed. (Academic Press, London, 1986).
[7] J. E. Finn and P. A. Monson, Phys. Rev. A **39**, 6402 (1989).
[8] Y. Fan and P. A. Monson, J. Chem. Phys. **99**, 6897 (1993).
[9] E. Velasco and P. Tarazona, Phys. Rev. A **42**, 2454 (1990); J. E. Finn and P. A. Monson, *ibid.* **42**, 2458 (1990).
[10] Y. Fan, J. E. Finn, and P. A. Monson, Fluid Phase Equilib. **75**, 163 (1992).
[11] S. Sokolowski and J. Fischer, Phys. Rev. A **41**, 6866 (1990).
[12] J. D. Weeks, D. Chandler, and H. C. Andersen, J. Chem. Phys. **54**, 5237 (1971).
[13] Y. Rosenfeld, Phys. Rev. Lett. **63**, 980 (1989); E. Kierlik and M. L. Rosinberg, Phys. Rev. A **42**, 3382 (1990); S. Phan, E. Kierlik, M. L. Rosinberg, B. Bildstein, and G. Kahl, Phys. Rev. E **48**, 618 (1993).
[14] J. A. Barker and D. Henderson, J. Chem. Phys. **47**, 4714 (1967).
[15] B. Q. Lu, R. Evans, and M. M. Telo da Gama, Mol. Phys. **55**, 1319 (1985).
[16] J. P. R. B. Walton and N. Quirke, Chem. Phys. Lett. **129**, 382 (1986).
[17] S. Nordholm, M. Johnson, and B. C. Freasier, Aust. J. Chem. **33**, 2139 (1980); M. Johnson and S. Nordholm, J. Chem. Phys. **75**, 1953 (1981).
[18] P. Tarazona and R. Evans, Mol. Phys. **52**, 847 (1984); P. Tarazona, Phys. Rev. A **31**, 2672 (1985); Z. Tan, G. S. Gubbins, U. Marini Bettolo Marconi, and F. van Swol, J. Chem. Phys. **90**, 3704 (1989).
[19] W. A. Curtin and N. W. Ashcroft, Phys. Rev. A **32**, 2909 (1985); A. R. Denton and N. W. Ashcroft, *ibid.* **42**, 7312 (1990).
[20] F. van Swol and J. R. Henderson, Phys. Rev. A **43**, 2932 (1991).
[21] See, A. Kol and B. B. Laird, Mol. Phys. **90**, 951 (1997), and references therein.
[22] Y. Rosenfeld, M. Schmidt, H. Lowen, and P. Tarazona, J. Phys.: Condens. Matter **8**, L577 (1996); Phys. Rev. E **55**, 4245 (1997).
[23] P. Tarazona, Phys. Rev. Lett. **84**, 694 (2000).
[24] M. B. Sweatman, Mol. Phys. **98**, 573 (2000).
[25] C. Ebner and W. F. Saam, Phys. Rev. Lett. **38**, 1486 (1977); W. F. Saam and C. Ebner, Phys. Rev. A **17**, 1768 (1978).
[26] J. E. Lane, T. H. Spurling, B. C. Freasier, J. W. Perram, and E. R. Smith, Phys. Rev. A **20**, 2147 (1979); T. F. Meister and D. M. Kroll, *ibid.* **31**, 4055 (1985).
[27] G. Mistura, F. Ancilotto, L. Bruschi, and F. Toigo, Phys. Rev. Lett. **82**, 795 (1999).
[28] J. Kolafa and I. Nezbeda, Fluid Phase Equilib. **100**, 1 (1994).
[29] A. Z. Panagiotopoulos, Mol. Phys. **61**, 813 (1987); A. Z. Panagiotopoulos, N. Quirke, M. Stapleton, and D. J. Tildesley, *ibid.* **63**, 527 (1988); D. Frenkel and B. Smit, *Understanding Molecular Simulation* (Academic Press, New York, 1996).
[30] Y. Rosenfeld, J. Chem. Phys. **98**, 8126 (1993).
[31] M. P. Allen and D. J. Tildesley, *Computer Simulation of Liquids* (Oxford University, New York, 1987).
[32] J. J. Nicolas, K. E. Gubbins, W. B. Street, and D. J. Tildesley, Mol. Phys. **37**, 1429 (1979).
[33] *Handbook of Chemistry and Physics*, edited by D. R. Lide, 74th ed. (CRC Press, Boca Raton, 1993).
[34] For example, see S. C. Kim and P. T. Cummings, Mol. Phys. **99**, 1099 (2001); S. Zhou, Phys. Rev. E **63**, 061 206 (2001).
[35] M. Schmidt, J. Phys.: Condens. Matter **11**, 10 163 (1999); Phys. Rev. E **62**, 3799 (2000); **62**, 4976 (2000).
[36] J. A. Cuesta and Y. Martinez-Raton, J. Chem. Phys. **107**, 6379 (1997); **111**, 317 (1999).